Program Digest, 2019 IEEE International Ultrasonics Symposium (IUS)
Glasgow, Scotland, October 6-9, 2019

Compartment Syndrome Detection Using Vibration-Enabled Ultrasound Shear Wave Elastography – Simulation and Experimental Results

Man M Nguyen
Philips Research North America
Cambridge, MA, USA
man.nguyen@philips.com

Ramon Erkamp
Philips Research North America
Cambridge, MA, USA

Hua Xie
Oregon Health & Science University
Portland, OR, USA

Meihua Zhu
Oregon Health & Science University
Portland, OR, USA

Todd Graham
Oregon Health & Science University
Portland, OR, USA

Jack Lazar
Oregon Health & Science University
Portland, OR, USA

James M Jones
Oregon Health & Science University
Portland, OR, USA

Cynthia R Gregory
Oregon Health & Science University
Portland, OR, USA

Sean Kyne
Philips Research North America
Cambridge, MA, USA

Vijay Shamdasani
Philips Healthcare
Bothell, WA, USA

Anthony Gades
Philips Healthcare
Bothell, WA, USA

Kenton W Gregory
Oregon Health & Science University
Portland, OR, USA

***Abstract*— Ultrasound shear wave elastography (SWE) has become a clinically accepted tool for tissue characterization, cancer diagnosis, and therapy assessment. However, it is only commercially available on premium ultrasound scanners and high-performance transducers capable of sustaining high-voltage, long-duration acoustic push-pulses. Mechanical vibration is an alternative method for acoustic radiation force (ARF) to induce shear wave propagation inside soft tissue, thus enabling ultrasound SWE on low-cost and portable systems. One potential application is compartment syndrome (CS), with the acute cases commonly seen in traumatic injuries and chronic cases caused by exercise injuries. CS is a condition in which the increased pressure in the muscle compartment inhibits capillary blood flow and subsequently causes muscle ischemia. To avoid permanent muscle injury, CS must be diagnosed and treated rapidly. In this study, a vibration-enabled SWE prototype was implemented on a commercial scanner and evaluated using an *in vivo* swine CS model as a proof-of-concept for non-invasive CS detection.**

Keywords—ultrasound, shear wave elastography, vibration-induced shear-wave elastography, musculoskeletal, MSK, compartment syndrome

I. Introduction

A. Shear wave elastography (SWE)

Injured and diseased tissues have different mechanical properties compared to healthy counterparts. Shear wave elastography (SWE) refers to tissue stiffness quantification and imaging. SWE has become a clinically accepted diagnostic tool for tissue characterization, cancer diagnosis, and therapy assessment. Among different modalities, ultrasound-based SWE stands out because it offers advantages of real-time, low cost, and easy access [1-6]. Ultrasound SWE has been extensively investigated on liver, breast, prostate, and thyroid for cancer detection and disease assessment.

Ultrasound SWE requires complex circuitry and high power consumption and is thus only available on premium systems with high-performance ultrasound transducers. These systems are not practical in settings with constraints in space, mobility, and cost (i.e. emergency room, off-hospital clinics, and battlefield settings). Currently, there is no commercially available portable ultrasound imaging system capable of SWE. This limitation is due to the current method of generating in-tissue shear waves, which requires long, high energy, acoustic pulses. These so-called push pulses are 100-400 times longer than regular pulse used in ultrasound B-mode imaging. An alternative method for generating shear waves is to use external mechanical vibration. This alternative method does not involve the use of long, high energy, acoustic pulses for generating in-tissue shear waves, and thus may allow SWE to be implemented in low-cost, portable systems [5-11].

B. Compartment syndrome (CS)

Extremity wounds are one of the most common traumatic and disabling injuries for civilians as well as for soldiers on the battlefield and are frequently complicated by compartment syndrome (CS). CS magnifies the initial injury from fractures, crush injuries, extreme exertion, soft tissue infection, and prolonged tourniquet application, increasing the time to healing and utilization of health care resources, and decreasing the chance of a full functional recovery. CS is due to injury-related edema and swelling of muscle compartments that leads to abnormal increases in compartment pressure from normal (10-15 mmHg to $\geq$ 30 mmHg which is associated with cessation of capillary blood flow and ischemia. Loss of perfusion then results in ischemia and infarction of muscle, nerve, and vascular tissue, and an emergent surgical fasciotomy is required within three to six hours to relieve compartment pressure and re-establish blood flow. CS is a dynamic event with intra-compartment pressures developing with a different temporal profile in each patient so that serial measurements are frequently needed. The present clinical standard for diagnosis of extremity CS is a sterile, single-patient, single-use, needle-based pressure gauge (Stryker intra-compartmental pressure monitor). Despite an emergency surgical fasciotomy, infarction of tissue frequently results in incomplete tissue regeneration and healing that leads to long-term loss of nerve and muscle function. A non-invasive, safe device that can be used rapidly, simply and serially on one or more patients with an immediate accurate diagnosis of CS, could significantly improve the accuracy and timeliness of CS diagnosis in the hands of civilian emergency response personnel, combat medics, emergency department personnel and physicians, and lead to improved outcomes [12].

Several studies have shown that changes in muscle elasticity are correlated with the compartment pressure [13-14]. In this study, we investigated the use of ultrasound shear-wave elastography for diagnosing compartment syndrome in a swine model. An EPIQ (Philips Healthcare, Andover, MA) ultrasound scanner and an eL18-4 (Philips Healthcare) high-frequency linear transducer were used with two shear-wave generation methods: 1) the default acoustic radiation force and 2) an external mechanical vibrator. Finite Element Model (FEM) simulation and phantom experiments were performed to understand the behavior of shear waves generated by mechanical vibration and provide inputs for the prototype to be used *in vivo* experiments.

II. Methods

A. Simulation

Mechanical-vibration-enabled shear waves were simulated using FEM PZFlex with a variety of vibrator shapes and vibration patterns. These are full 3-D volumetric simulations (90 mm axial range, 160 mm lateral, 40 mm elevation) with a 0.4 mm^3 voxel size, on homogeneous isotropic linear medium with 10kPa (Young's Modulus) background. Side boundaries are absorbing while top medium surface is reflective and free moving. Probe contact area and bottom area have fixed nodes. Fig. 1 illustrates an example where an external vibrator (Fig. 1a) was compared against vibrating the probe itself (Fig. 1b) for shear wave generation. These configurations were described in previous academic work [6-9]. The external vibrator is modeled after commercially available paging vibrators that are based on an eccentric weight attached to a small motor (8 mm diameter, 8 mm long cylinder shape) vibrating at 140 Hz in a circular sinusoidal motion in the axial-lateral plane with a vibration amplitude of 0.57 mm, and 4 mm indentation into the medium. The linear transducer is also indented 4 mm into the medium, as a small push force would be needed to transfer probe vibration to tissue. The image shows the resulting shear wave (axial motion component on ±150 μm scale) after 44 ms. Near the vibrator, the motion exceeds the display range, larger than 150 μm motion, is indicated with the black and white colors. Fig. 1b depicts the case where the whole probe is vibrating with the same motion as the side vibrator. For the external vibrator (Fig. 1a), there is a preferential angular direction of shear wave propagation at about 40 degrees relative to axial for the propagation. For the whole probe vibration (Fig. 1b), there are complex interference patterns that depend on vibration frequency, probe shape, and YM distribution.

B. Design and prototype development

After evaluating the simulation results and considering the design complexity, a side-vibration-based prototype consisting of an off-the-shelf vibrator and a custom-made holder was attached to Philips linear 1D transducer eL18-4 (Fig. 2). The vibration is controlled by a function generator which provides the timing and duration of the vibration (140 Hz for 300 ms). A customized circuit board consisting of a voltage regulator and capacitors was used to shorten the ramping up and down periods of the vibrator. The setup is synchronized with an EPIQ system using the external frame trigger signal from EPIQ.

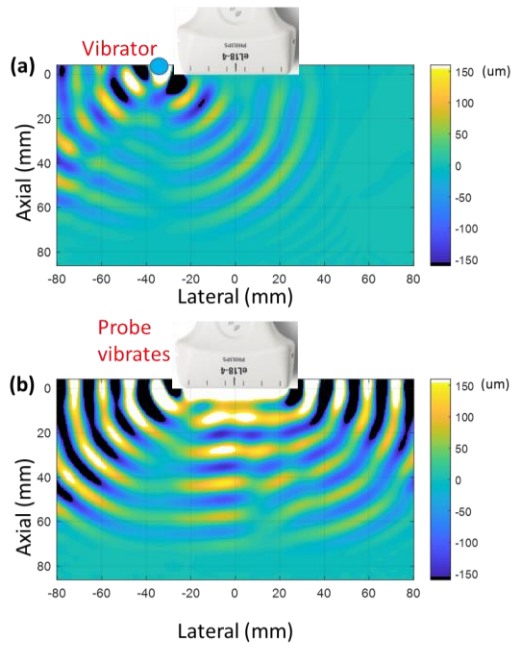

Fig. 1. Two examples of PZFlex simulation setups: (a) side vibration and (b) whole-probe vibration

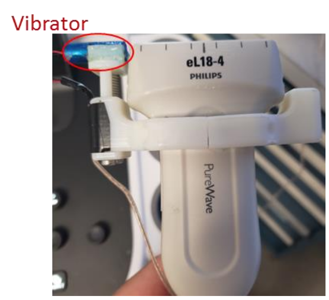

Fig. 2. Vibration-enabled shear wave elastography prototype with Philips eL18-4

C. Experiment

Desired shear wave propagation by mechanical vibration was confirmed on CIRS elasticity phantoms (CIRS, Norfolk, VA) and qualitatively compared with the simulation results before being used in the *in vivo* experiment (Fig. 3).

The *in vivo* study followed an IACUC-approved (Institutional Animal Care and Use Committee) protocol for creating CS in the anterior tibialis muscle (ATM) compartment of domestic swine. After sedation and placement on inhaled anesthesia, CS was induced by a unilateral ATM injury resulting from the infusion of autologous plasma into the anterior compartment of one leg. To measure compartment pressures, a Stryker Intra-Compartmental Pressure Monitor System (Stryker Instruments, Kalamazoo, MI) needle was inserted into the ATM compartment and the pressure was read from the digital display. SWE data were collected using both Philips commercial SWE product ElastQ with the default ARF push pulses and the mechanical vibration-enabled SWE prototype.

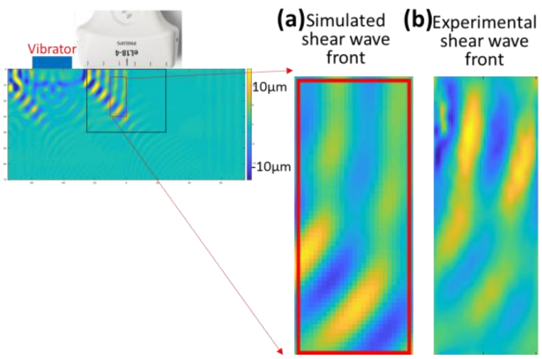

Fig. 3. Simulation vs. experiment validation: (a) Simulated shear wavefront; (b) Experimental shear wavefront. The displacement scales were normalized to observe the wavefront shapes.

III. Results

A. Simulation results

The experimental phantom results showed comparable shear-wave propagation patterns to the simulation results (Fig. 3). Fig. 4 shows the Young's Modulus (YM) reconstruction on simulated shear wave propagation for side vibrator (middle column) and whole probe vibration (right column). The first column shows the three medium scenarios being considered: homogeneous 10 kPa phantom (Fig. 4a), a 40 kPa flat layer from axial depth 10 mm to 30 mm (Fig. 4b), and a 40 kPa sloped wedge shape layer (muscle compartments are often wedge-shaped on ultrasound images) (Fig. 4c). These medium designs are intended to mimic the compartment syndrome condition where the muscle with elevated compartment pressure is expected to stiffen [13-14].

For the side vibrator configuration, there is a reasonable agreement between the reconstructed YM maps and the ground truth. The artifacts at the layer edges, also seen with the whole-probe vibration configuration, are due to a quantization effect from the relatively large 0.4 mm voxel size (artifact locations exactly coincide with voxel steps). Overall, the side vibrator configuration offers more uniform reconstructed YM maps compared to the whole-probe vibration configuration. These results can be explained by the interference patterns of the shear wave propagation. The relatively big vibration source (larger than a wavelength) leads to the near field constructive and destructive interference patterns inside the imaging field-of-view underneath the vibration source, resulting in localized artifacts seen in the whole-probe vibration. Based on the results and other considerations regarding the vibrator size and strength, we decided to perform further experiments with an external side vibrator instead of the whole probe vibration.

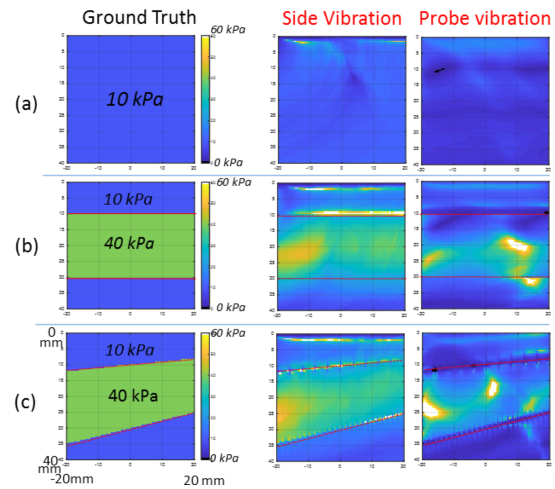

Fig. 4. Young's Modulus reconstruction from vibration-enabled shear wave simulation with three media for side vibration (middle column) and whole probe vibration (right column). The Young Modulus elasticity maps were reconstructed using wave equation [10].

B. Experimental results

Fig. 5 shows the SWE Young's Modulus maps overlaid on 2D real-time images of the longitudinal views of the anterior tibialis muscle using the default ARF push-pulse ElastQ for 2 swine models. These images were acquired at the baseline (normal) compartment pressure and at the elevated compartment pressure of 30-35 mmHg. The measurements based on the oval ROI on these muscles show a good correlation of Young's Modulus with the compartment pressure in both swine models: about 20-23 kPa at normal state and significantly increased to 33-48 kPa at the elevated compartment pressure ($\geq$ 30 mmHg). The increase in tissue stiffness can also be visualized with the elasticity color maps changing from blue-green in baseline cases to yellow-red in the CS cases with the 0-60 kPa dynamic range.

Similar results were obtained with the vibration-enabled SWE prototype (Fig. 6). However, higher spatial variations were observed in the CS cases with spotted red dots seen in the muscle. This is likely due to the changes in wavefront and interference patterns as it propagates through non-homogenous media of stiffened muscles.

Fig. 7 plots stiffness measurements on normal and CS muscles using both ARF and vibration-enabled SWE methods. These averages and standard deviations in the figures were calculated based on three measurements (oval ROIs on the ATM) on different images acquired at each state for each animal. For both ARF SWE and vibration-enabled SWE, the elasticity difference from normal to >30 mmHg in each ATM compartment was significantly different ($p<0.001$, two-tailed t-test). While there is some agreement with ARF SWE, vibration-enabled SWE seems to have challenges with stiffened muscle, resulting in either high variation (in Animal 2) or large discrepancy compared to ARF SWE (in Animal 1).

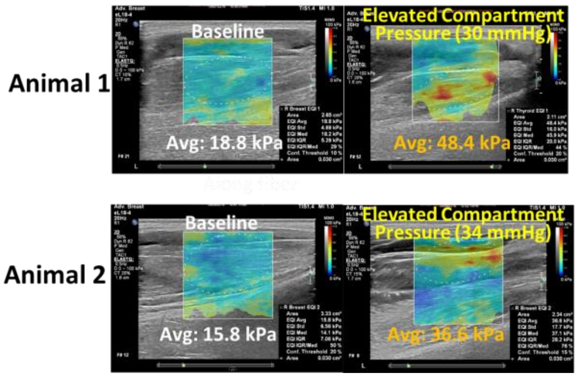

Fig. 5. Experimental results using the default ARF push-pulse ElastQ on anterior tibialis muscle with normal compartment pressure (left column) and elevated compartment pressure (right column)

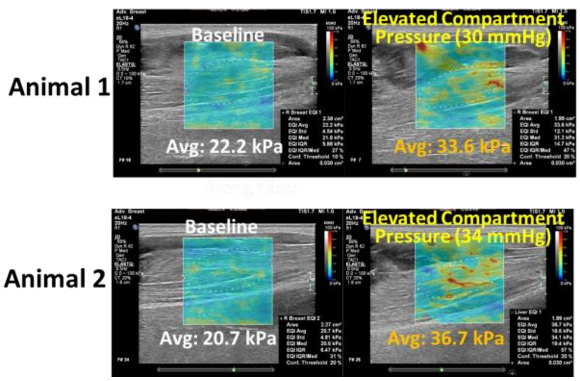

Fig. 6. Experimental results using the vibration-enabled SWE prototype on anterior tibialis muscle with normal compartment pressure (left column) and elevated compartment pressure (right column).

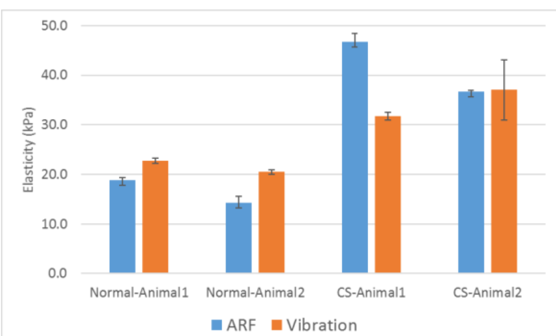

Fig. 7. Means and standard deviations (n=3) of Young's Modulus measurements on normal and CS muscle using ARF and vibration-enabled SWE. For each method and animal, the elasticity difference from normal to > 30 mmHg in the ATM compartment was significantly different ($p<0.001$, two-tailed t-test).

IV. Conclusion

In this study, we demonstrated the potential use of shear wave elastography for a simple, fast, and accurate diagnosis of compartment syndrome. There is a highly significant difference in elasticity measurements between normal compartment pressures and pressures > 30 mmHg, indicating compartment syndrome. This diagnosis can also be visually achieved by the elasticity maps.

The results show the potential use of vibration-enabled SWE in systems incapable of generating and withstanding high-power, long acoustic push-pulses. These findings suggest the potential of vibration-enabled SWE for CS detection. While the off-line analysis further demonstrated that tissue displacement induced by the vibration-enabled SWE prototype is one order of magnitude larger than the counterpart by ARF ElastQ, more investigation is needed to overcome the challenges of distorted wavefronts (in shapes and amplitudes) as well as repeatability to bring the vibration-enabled SWE to clinics.

References

[1] Ferraioli G, Parekh P, Levitov AB, Filice C. Shear wave elastography for evaluation of liver fibrosis. J Ultrasound Med. 2014 Feb;33(2):197-203.

[2] Foucher J, Chanteloup E, Vergniol J, Castera L, Le Bail B, Adhoute X, Bertet J, Couzigou P, and Ledinghen V. Diagnosis of cirrhosis by transient elastography (Fibroscan): a prospective study, Gut, vol. 55, no. 3, pp. 403408, 2006.

[3] Azizi G, Keller JM, Mayo ML, Piper K, Puett D, Earp KM, Malchoff CD. Thyroid Nodules and Shear Wave Elastography: A New Tool in Thyroid Cancer Detection. Ultrasound Med Biol. 2015 Nov;41(11):2855-65.

[4] Liu BJ, Li DD, Xu HX, Guo LH, Zhang YF, Xu JM, Liu C, Liu LN, Li XL, Xu XH, Qu S, Xing M. Quantitative Shear Wave Velocity Measurement on Acoustic Radiation Force Impulse Elastography for Differential Diagnosis between Benign and Malignant Thyroid Nodules: A Meta-analysis. Ultrasound Med Biol. 2015 Dec;41(12):3035-43.

[5] Zippel D, Shalmon A, Rundstein A, Novikov I, Yosepovich A, Zbar A, Goitein D, Sklair-Levy M.Freehand elastography for determination of breast cancer size: comparison with B-mode sonography and histopathologic measurement.J Ultrasound Med. 2014 Aug;33(8):1441-6.

[6] Yamakoshi Y, Sato J, Sato T.Ultrasonic imaging of internal vibration of soft tissue under forced vibration. IEEE Trans Ultrason Ferroelectr Freq Control. 1990;37(2):45-53.

[7] Zhao H, Song P, Meixner DD, Kinnick RR, Callstrom MR, Sanchez W, Urban MW, Manduca A, Greenleaf JF, Chen S. External vibration multi-directional ultrasound shearwave elastography (EVMUSE): application in liver fibrosis staging. IEEE Trans Med Imaging. 2014 Nov;33(11):2140-8.

[8] Mellema DC, Song P, Kinnick RR, Urban MW, Greenleaf JF, Manduca A, Chen S. Probe Oscillation Shear Elastography (PROSE): A High Frame-Rate Method for Two-Dimensional Ultrasound Shear Wave Elastography. IEEE Trans Med Imaging. 2016 Sep;35(9):2098-106.

[9] Yang H, Nguyen M, Huang SW, Shamdasani V, Xie H, Anthony BW. Simulation, design, and implementation of external mechanical vibration for ultrasound shear wave elastography. Ultrasonics Symposium (IUS), 2017 IEEE International, 1-4

[10] Bercoff J, Chaffai S, Tanter M, Sandrin L, Catheline S, Fink M, Gennisson JL, Meunier M. In vivo breast tumor detection using transient elastography. Ultrasound Med Biol. 2003 Oct;29(10):1387-96.

[11] Belmont PJ Jr, McCriskin BJ, Sieg RN, Burks R, Schoenfeld AJ. Combat wounds in Iraq and Afghanistan from 2005 to 2009. J Trauma Acute Care Surg. 2012 Jul;73(1):3-12.

[12] McMillan TE, Gardner WT, Schmidt AH, Johnstone AJ. Diagnosing acute compartment syndrome-where have we got to? Int Orthop. 2019 Aug 29.

[13] Brandenburg JE, Eby SF, Song P, Zhao H, Landry BW, Kingsley-Berg S, Bamlet WR, Chen S, Sieck GC, An KN. Feasibility and reliability of quantifying passive muscle stiffness in young children by using shear wave ultrasound elastography. J Ultrasound Med. 2015 Apr;34(4):663-70.

[14] Lacourpaille L, Hug F, Bouillard K, Hogrel JY, Nordez A. Supersonic shear imaging provides a reliable measurement of resting muscle shear elastic modulus. Physiol Meas. 2012 Mar;33(3):N19-28.